Title

A New Year's Day Icebreaker: Icequakes on Lakes in Alberta, Canada

Authors

Jeffrey Kavanaugh[1]

*Ryan Schultz[2]

Laurence Andriashek[2]

Mirko van der Baan[1]

Hadi Ghofrani[3]

Gail Atkinson[3]

Daniel J. Utting[2]

[1] University of Alberta, Edmonton, Alberta

[2] Alberta Geological Survey, Edmonton, Alberta

[3] Western University, London, Ontario

*Corresponding Author: Ryan.Schultz@aer.ca

Accepted in the Canadian Journal of Earth Sciences

doi: 10.1139/cjes-2018-0196.

Abstract

Any process that causes a sudden brittle failure of material has the potential to cause earthquake-like seismic events. Cryoseisms represent an underreported class of seismic event due to their (often) small magnitudes. In this paper, we document the phenomenon of some of the largest magnitude lake-associated icequakes (M_L 2.0) yet reported. These events occurred nearly simultaneously (within ~2 hours) on geographically separate lakes in Alberta, Canada starting January 1 2018. We conjecture that these events were caused by the sudden brittle failure of lake ice due to thermal expansion; the effects of the thermal expansion were compounded by the lack of insulating snow cover, high lake water levels, and a rapid onset of atmospheric warming. These factors also contributed to ice-jacking – a repeating process in which thermal contraction produces tensile cracks (leads) in lake ice that are then filled with water that is frozen during the cooling cycle. Thus, any subsequent thermal expansion must be accommodated by new deformation or brittle failure. This ice-jacking process caused creeping ground deformation after the initial brittle failure and again two weeks later following a second warming period. In many cases, the resulting ground deformation was significant enough to cause property damage.

Key Words

Icequakes, Lakes, Iceheave, Cryoseisms, Alberta

1 Introduction

Cryoseisms are a class of seismic event that has garnered increased attention in recent years (Podolskiy & Walter 2016; Aster & Winberry, 2017). Understandably, the major part of this attention has been focused towards large glacier systems given the information seismic signals can provide about ice dynamics (e.g. Anandakrishnan & Bentley, 1993; Stuart et al., 2005), hydrological forcing (e.g. Walter et al., 2008), and iceberg calving (e.g. Qamar, 1988; Amundson et al., 2008). More broadly, the cryosphere has the potential to generate seismic events in any region where ice-dominated materials ranging from frozen soils to glacial ice experience thermal, phase change, gravitational, or other stresses that lead to fracture or other strain-weakening failure. For example, a particular subset of events known as frostquakes occur in regions that undergo rapid freezing (and volumetric expansion) of ground water (Barosh, 2000; Nikonov, 2010); this phase change causes a rapid increase in stress that is suddenly released, causing cracking and heaving deformations of the ground surface (Battaglia et al., 2016). Often, these events are of a sufficiently small magnitude to go unnoticed, even by sensitive seismic networks. Instead, detection may rely on citizen reporting for improved consistency (Leung et al., 2017).

Even more obscure than frostquakes are cryoseisms that occur near standing bodies of frozen water, such as lakes (Bradley, 1948; Hamaguchi et al., 1977; Nishio, 1983; Ruzhich et al., 2009). In these events (similar to some types of events that occur on glaciers), seismic motions result from the sudden brittle failure of lake ice due to thermal expansion stresses (Goto et al., 1980). Seismic events of this type have been studied as a small analogue for crustal scale processes (Hamaguchi & Goto, 1978; Dobretsov et al., 2007; 2013). In some cases, these brittle failures can be sudden and large enough to be considered as a source of seismic hazard to infrastructure (Makkonen et al., 2010).

Here, we document a series of suspected lake-associated icequakes of moderate magnitude (~2.0 M_L) that occurred on the evening of January 1-2 2018 in central Alberta, Canada. In this paper, we detail seismological phenomena including hypocentres, timings, magnitudes, and likely ground motions and compare these with felt reports. Furthermore, we bolster these data with onsite observations of ground deformations, fissures, and ice ridges associated with the suspected icequakes. These ground deformations continued to (aseismically) grow in the weeks following the initial icequakes. Based on these observations, we discuss the causal meteorological factors thought to be associated with the genesis of these icequakes. Finally, we consider the implications our interpretations have for the paucity of recorded cryoseismic events and the potential for larger magnitude events to occur on lakes in Alberta. Recognition of these types of events is important, especially to distinguish them from the induced seismic events that are prevalent in the Western Canada Sedimentary Basin (Atkinson et al., 2016; Schultz et al., 2017; 2018).

2 Seismological Observations

2.1 Event Recordings

During the night of January 1-2 2018, a large number of anomalous shaking incidents were simultaneously felt in the municipalities nearby Lac Ste. Anne, Alberta. Residents reported being woken by loud boom/popping sounds and shaking intense enough to rattle homes and the shelves/cupboards within. One noteworthy report from a resident's guest (visiting from

California and familiar with the type of motion) described the shaking as “exactly like an earthquake.” The following morning, newly created fissures, ridges, and cracks in the ice/ground were apparent – some coupled with damage to property. These incidents were circulated through various media outlets (e.g., Global News, 2018), creating widespread public interest in the subject. Following this, a series of “us too” felt shaking and ground deformation reports were sent into the Alberta Geological Survey (AGS) and the University of Alberta. A significant number of these reports hailed from municipalities nearby other lakes in central Alberta.

These felt reports were received in conjunction with the detection and location of seismic events on the evening of January 1-2 2018. Seismic events are routinely catalogued at the AGS (Stern et al., 2013) from real-time, publicly-available waveform data (e.g., Schultz & Stern, 2015). Given the interest on the felt reports of January 1-2 2018, waveform data from that evening were carefully reviewed by visual scanning (assuming a location from Lac Ste. Anne) and then reanalyzed. Three earthquake-like events were recognized in this dataset, all of which were located coincident with lakes in the centre of the province (Figure 1). Two of these events, on Pigeon Lake and Lac Ste. Anne, geographically corroborate felt reports. Furthermore, the timing for the reports at Pigeon Lake (~23:45 MST) is nearly simultaneous with the detected event (23:47 MST = 6:47 UTC). However, the only seismically discernible event from Lac Ste. Anne occurs prior (23:06 MST) to the nearly unanimous set of felt report timings (1:30 MST). We note that the low magnitude of these events (~2.0 M_L) is near the detection threshold for the region (Schultz et al., 2015; Cui & Atkinson, 2016).

Despite complexities associated with locating small magnitude events, hints of additional (unlocatable) seismic events are apparent in the data. To demonstrate this, we time shift the waveform data of horizontal components for nearby stations (Figure S1); this process aligns the largest amplitude phase arrivals from a given origin to be contemporaneous. After these shifts, numerous cases of seismic event-like arrivals originating from lakes are apparent. This likely represents the fact that the located events are simply the most discernable in an ongoing sequence originating from these lakes, continuing throughout the evening of January 1-2 2018. In fact, small magnitude seismic events related to ice cover could contribute to a background source of coherent noise (Gu & Shen, 2012).

2.2 Ground Motions and Shaking Intensity

Small magnitude seismic events were identified at three central Alberta lakes: Lac Ste. Anne, Gull Lake, and Pigeon Lake. To assess the propensity for these events to cause noticeable shaking or potential damage, we compiled a ground motion database of pseudo-spectral acceleration (PSA) from the signals recorded on nearby stations. Briefly, the velocity waveforms are corrected, filtered, and then deconvolved from instrument response (see methods in Assatourians and Atkinson, 2010). Peak ground velocity (PGV) and peak ground acceleration (PGA) values are computed from the maximum amplitudes of processed waveforms. PSAs are calculated from the processed acceleration waveforms following the Nigam and Jennings (1969) formulation for the computation of 5% damped response spectra.

Additionally, we qualitatively compare the waveforms and spectra of the Lac Ste. Anne event against a small-magnitude natural event (M_L 0.7) and other small cryoseisms (M_L -0.2 to 1.4) in Alberta (Figure S2). This series of seismic events were detected around the Brazeau River and reservoir starting in 2014, and are likely cryoseisms based on their waveform characteristics and timing (Ghofrani & Atkinson, 2018). We note that waveforms from the event on Lac St Anne are more similar to the waveforms of the Brazeau-area cryoseisms (in terms of waveform shape, duration, and frequency content) than to those of the small-sized natural event. These observations become more quantitatively apparent when comparing the displacement spectra of the Lac Ste. Anne event against a Brazeau-area cryoseisms and earthquake (Figure 2). From this figure it can be observed that the Lac St. Anne event has lower power at high frequencies as compared to the small, natural event. Compared with the Brazeau cryoseisms, the event at Lac Ste. Anne is similar in frequency content. It should be noted that the background microseism noise level in the Brazeau area is high at frequencies lower than 1 Hz, causing the pronounced spectral peak at 0.2 Hz.

Having determined the specific locations and times of the three lake events of January 1-2 2018, we fit their PSA, PGA, and PGV into regional ground motion prediction equations (GMPEs) to infer the near-source shaking. We use the A15 (Atkinson & Assatourians, 2017) and MK17 (Mahani & Kao, 2017) GMPE models, which were developed for **M**>3.0 and MK17 is developed for **M** 1.5-3.8 events, respectively. However, the magnitudes of the three recent events are smaller than **M** 3.0 (M_L~2.0) and have different frequency content than do similarly-sized earthquakes (Figures S2 & 2). As well, the GMPEs are for the horizontal-component of motion on a soft-rock site condition (760 m/s) – the recording sites are on softer soils and may amplify the horizontal components significantly. We therefore consider only the vertical component of recorded motion, as a proxy for the unamplified horizontal component (since vertical components are not as affected by site response (Lermo & Chavez-Garcia, 1993; Siddiqqi & Atkinson, 2002; Atkinson & Boore, 2006). For these reasons, we caution that our use of these GMPEs is only as an approximate (but best available) guide.

Despite these complications, we compared PSA (at 1.0 and 3.3 Hz) and PGA values of the three events against the AK15/MK17 GMPE expected values (Figure 3). We find that GMPE expected values (at < 100 km and **M** ~2.1) are consistent with the data at 1.0 Hz. Based on the recorded ground motions and the GMPEs, we are thus able to extrapolate the expected near-source (1 km) motions. To next translate the near-source motions to Modified Mercalli Intensity (MMI) we use a conversion equation (Atkinson & Kaka, 2007). Input near-source PGA/PGV values and converted MMIs for the three lake events are given in Table 1.

Table 1. The estimated MMI values using empirical conversion equations.

Lac Ste. Anne Event (**M**~2.2)			Gull Lake Event (**M**~2.0)			Pigeon Lake Event (**M**~2.1)		
PGA/PGV (at 1 km)	MMI[1]	MMI[2]	PGA/PGV (at 1 km)	MMI[1]	MMI[2]	PGA/PGV (at 1 km)	MMI[1]	MMI[2]
6.572 0.104	3.8	3.1	4.447 0.068	3.6	2.8	5.406 0.084	3.7	3.0

MMI[1] and MMI[2] represent the calculated intensities using PGA (cm/s^2) and PGV (cm/s), respectively.

The estimated/extrapolated MMIs in municipalities are between III-IV and related to "weak" levels of ground shaking (Table 1). Often, shaking of this intensity is felt quite noticeably by persons indoors, especially on upper floors (Wood et al., 1931). Additionally, stationary vehicles may rock slightly given "weak" ground shaking. These intensities are roughly consistent with felt reports from an icequake on Lake Mendota, Wisconsin (Bradley, 1948) where people were awakened from their sleep and noted the rattling of their homes. However, the computed MMIs and near-source ground motions themselves are likely of insufficient strength to cause the reported damage to nearby property. Instead, another mechanism is likely responsible for the observed damage to infrastructure.

3 Ground and Ice Deformation Observations

Because west-central Alberta is not prone to seismic activity (Stern et al., 2013), a field investigation was initiated (January 4-5 2018) to verify the nature of the M_L 2.0 seismic events. Observations of both ice and ground deformation were recorded by AGS at Pigeon and Lac. Ste. Anne; documentation of similar disturbances was made by cottage-owners at Wabamun Lake and Baptiste Lake and was provided to AGS for analysis. Initial media coverage focused mainly on damage to infrastructure along the shoreline of Lac. Ste. Anne (Global News, 2018). AGS visited four sites along the southeast shore of Lac. Ste. Anne (Sunset Beach, Alberta Beach, Val Quentin, Thibeault, Figure 1b) on January 4-5, and then re-visited some of those sites two weeks later on January 18-19. An additional site (Ross Haven) was visited approximately one month after the seismic event. The following describes these observations, as well as anecdotal comments by cottage owners on that night – many of whom had never encountered anything like this in the handful of decades living on the lakeshore.

3.1 Ice Ridges

Around 23:45 MST January 1, cottage owners at Pigeon Lake (Figure 1d) were alarmed by an explosive sound, with some rushing out of their homes to inspect for damage. The next morning, a view of what happened was apparent: the flat lying lake surface of the previous day had become a 1-2 m high ice ridge extending ~500 m parallel to the shoreline (at about 8-10 m offshore). An AGS visit to Mulhurst Bay (Pigeon Lake) on January 4 observed that slabs of ice were thrust nearly vertically into ice ridges, with as much as 3-4 m of shortening (Figure 4a). Elsewhere, the ice ridge was expressed as finger rafts (Government of Canada Ice Glossary) of alternating over and under thrust slabs of ice (Figure 4b). Inclusions of boulders frozen to the base of some thrust slabs on the opposite side of the lake indicated that ice had frozen to its bed prior to the development of the ice ridge (Figure 4a). No evidence of ground deformation was observed nor were there any known reports of damage to infrastructure. Local reports indicated ice ridges developed elsewhere in Pigeon Lake, but these were not examined by AGS. Like most of the west-central region of Alberta, snow cover in the area around Pigeon Lake at the time of investigation was thin: either entirely absent or sparse, but nowhere more than 10 cm deep.

Similar to Pigeon Lake, ice ridges were observed on January 5 along the southeast end of Lac. Ste. Anne. One major ridge developed near a public pier at Alberta Beach, extending northeast for a distance of about 600 m to Sunset Beach (Figure 1b). The height of the ridge was about 1.0-1.5 m; in many places it consisted of two near-vertical limbs of a ruptured fold, with as much as 3 m of shortening (Figure 4c). The southern end of the ridge near the pier extended almost 100 m offshore, but its position at the northern end was within 8-10 m of shoreline. A revisit to Sunset Beach on January 18 (2.5 weeks after the initial event) saw an approximate doubling of ridge height, increasing it by at least another metre (Figure 4d). This indicates that the ice ridge building processes were still active following the January 1 event. Further southwest of Alberta Beach, a similar sized ice ridge formed close to the shoreline, in numerous places ramping directly onshore (Figure 4e). The full extent of offshore ice ridges on Lac Ste. Anne is not fully known as the lake was not surveyed in its entirety.

Evidence of similarly styled ice ridges in the ice were documented at Wabamun Lake by a member of the local watershed management council, who provided ground-based and unmanned-aerial-vehicle (UAV) photos of numerous segments of the north shore of the lake (Figure 1). Offshore ice ridges or ruptured ice were recorded at only a few places at Wabamun Lake, primarily along the western shore at Seba Beach (Figure 4f). The largest of these were generally close to shore (3-5 m), not more than 1 m in height, and extending not more than 100 m in length.

3.2 Ground Deformation and Displacement

By far the biggest impact of the icequake event was the deformation and/or displacement of frozen ground along the shorelines of Lac Ste. Anne and Wabamun Lake. Deformation occurred in the form of thrusted, folded and overturned folded slabs of frozen ground, about 0.4 m thick, extending along shorelines for segmented distances of kilometres (Figure 5). These deformations were observed at many locations around Lac Ste. Anne, and along much of the west and north shoreline of Wabamun Lake. At Lac Ste. Anne, thrust slabs were observed to grow in height from initially about 1 m (January 5 2018) to as much as 2.5 m in the weeks following the seismic event (Figure 5 a,b,c). Conspicuously evident was the inverse relationship between the occurrence of offshore ice ridges and onshore ground deformation; in almost all cases where significant ground deformation occurred (with the exception of ice-ramping at Alberta Beach) lake ice was undeformed up to the shoreline; no evidence of ice ridge development was apparent (Figure 5 d,e) other than subtle downward warping beneath the displaced thrust sheets (Figure 5c). Conversely, ground deformation was not observed in those areas where ice ridges developed offshore. Associated with flat, undeformed lake ice were a number of offshore ice leads, some showing multiple opening and refreezing cycles. The significance of these to the creation of ground deformation and displacement is discussed later.

Of particular note was the occurrence of ground deformation in the form of multiple folds, rather than thrusts (Figure 6). Folds at the Thibeault site at Lac Ste. Anne occurred in flat terrain situated on the margins of a wetland where sediments were highly saturated prior to freeze-up (based on comments by the landowners in the area). Ground folds at Thibeault were observed as much as 25 m inland from the shoreline, and grew to a height of about 0.5 m during the 24 hours following the seismic event on January 1, (Figure 6b). By January 19 (2.5 weeks later) the height of these folds grew an additional metre, causing most to rupture along their fold axis (Figure 6 c,d). Similar inland folded terrain was observed from UAV imagery at a number of locations along Seba Beach on the western end of Wabamun Lake. Based on cracks visible in the snow cover, some folds appear to have ruptured shortly after their formation (Figure 6 e,f).

3.3 Damage to Infrastructure

The greatest issue property owners faced at Lac. Ste. Anne and Wabamun Lake (e.g., Wabamun Watershed Management Council Website, 2018; Don Meredith Outdoors Blog, 2018) was the widespread damage to buildings and other shoreline infrastructure that occurred following the seismic event (Figures 7 & S3). Initial damage to infrastructure took many forms, some of which could be related directly to ice or ground deformation. For example, upheaval of external building structures occurred beneath the Thibeault thrust folds (Figure 7 a,b) and damage to landscaping and other structures along shore were evident at Sunset Beach at Lac. Ste. Anne and Seba Beach at Wabamun Lake (Figure 7d). Ramping of an ice ridge onto shore at Alberta Beach caused deformation of decking and dislocation of buildings from their foundations (Figure 7c). However, in the Val Quentin area, horizontal dislocation of decking/buildings from their foundations (Figures S3 a,b) and compression/crushing of concrete foundations occurred in areas where expressions of either ice ridges, or significant ground deformation were not visible (Figure S3 c). These forms of structural damage occurred inland from the shoreline, much in the same manner that ground folds developed inland from the shoreline at Thibeault and Seba Beach (Figures 5 & 6). Damage to infrastructure was not confined to just the brief period following the seismic event, however. There was sustained damage that occurred in the few weeks following the initial event, as ground folds continued to grow (Figure 7 a,b).

3.4 Relationship to Ice Thickness and Lake-Bed Morphology

The observation of lake-bed sediments frozen to the underside of thrust ice slabs in some ice ridges (Figure 4a), and the absence of ice ridges in areas where ground deformation was severe (Figure 5), suggested that the occurrence and location of offshore ice ridges and onshore ground deformation may have been influenced by the nature of contact of lake ice with the underlying lake bottom. Four Ground Penetration Radar (GPR) transects were run from lake to shore at Lac Ste. Anne, two and half weeks after the seismic event, to test the relationship between ice thickness, depth to lake bottom, amount of free water between the ice and lake bottom, and ice ridge location. This method has been used previously to map bathymetry of lakes through ice (e.g. Annan and Davis 1977; Moorman and Michel 1997; Isaac and MacCulloch 2003). For this survey a Mala Ground Explorer GPR with a 160 MHz shielded antenna was used, pulled on a sled.

Transects 1 and 2 were both located near Sunset Beach on the east end of Lac. Ste. Anne (Figure 1b). Transect 1 terminated at the western, offshore edge of an ice ridge located about 6-7 m from the shoreline (Figures 4c,d, & 8). Transect 2, located about 500 m directly north of transect 1, terminated directly onshore where, although ice ridges were absent, there was significant ground deformation (Figures S2d & 5). Transects 3 and 4 were located about 100 m apart at Thibeault in the western part of Lac Ste. Anne (Figures 1b & S4), both located in an area where offshore ice ridges were absent, but where severe ground deformation occurred along the shoreline (Figures 5a-c & S4). Data from each GPR transect were calibrated with sounding information collected from ice-auger boreholes located along the transect trace in which ice thickness, depth to lake bottom, and amount of free water were recorded.

Depth soundings taken along GPR transect 1 showed that as the lake bottom rose toward shore, the depth of free water beneath the ice decreased from about 2.2 m to 0.2 m beneath the western edge of the ice ridge (Figure 8). Satellite imagery (Google Earth, 2011) taken mid-summer in the eastern part of the lake reveals highly reflective depositional bedforms beneath water near shore, suggesting the material is likely sand. When lake ice was penetrated by auger at the edge of the ice ridge, water flowed to surface for more than 15 minutes, indicating over-pressured conditions. In contrast, an auger hole located on the opposite side of the ridge, a distance of about 3.0-3.5 m, encountered no free water indicating that lake ice was frozen directly to its bed in the span between the ridge and shoreline.

GPR transect 2 terminated within a metre of the shoreline, where flat, undeformed lake ice abutted to thrusted and folded ground. A lake-depth sounding taken within less than a metre of the shoreline showed that ice was floating on at least 0.1 m of free water. Multiple refrozen ice cracks, or leads, were also conspicuous tens of metres away from, but parallel to, the shoreline (Figure 5d).

GPR Transects 3 and 4 both terminated at the shoreline, though the boundary between the lake and the marshy shoreline in this part of the lake was poorly defined. Numerous frozen leads, approximately 10-15 cm width, were encountered in both transects, the presence of which are expressed as the hyperbolic reflectors (Figure S4). Auger depth soundings indicate the presence of free water to within less than a metre of the ice-shoreline interface, with evidence of free water rising to surface at the boundary (Figure 5c).

4 Meteorological Observations

4.1 Weather Conditions Prior to January 1 2018

Here we discuss weather conditions preceding the seismic events of January 1 2018 detected at Lac Ste. Anne, Gull Lake, and Pigeon Lake. The nearest automated weather station to Lac Ste. Anne for which data are available is Alberta Agriculture and Forestry's Glenevis AGCM, located 11.5 km NNE of the lake and ~21 km NNE of Alberta Beach at 53°50'N 114°32'W. The air temperature record for this station (Figure 9) indicates that cold conditions persisted between December 29 and January 1, with temperatures ranging between -32.5°C and -22.3°C and averaging -29.0°C. During the 24 hours preceding the seismic event at 23:06 MST (6:06 UTC) on January 1, air temperatures increased from -29.4°C to -0.7°C, a +28.4°C warming. Over the same 24 hour period, hourly averaged wind speeds increased from 3.7 km/hr to 21.6 km/hr (including a jump of 15 km/hr immediately preceding the seismic event; with the wind veering from South to West (Figure S5a) over the course of the night.

The Alberta Agriculture and Forestry weather stations nearest to Pigeon and Gull lakes, respectively, are the St. Francis AGCM (located 27 km to the NNW at 53°18'N 114°19'W) and Leedale AGCM (located 26 km W at 52°33'N 114°28'W). Air temperature values recorded by the St. Francis AGCM (Figure 9) are similar to those observed near Lac Ste. Anne, ranging between -31.6°C and -21.7°C during the days prior to January 1, and a warming of +24.1°C was recorded over the 22 hour period preceding the 23:47 MST (6:47 UTC) seismic event detected at Pigeon Lake. Air temperatures recorded by the Leedale AGCM were slightly lower, ranging between -35.6°C and -24.7C over the December 29–January 1 interval (Figure S5b), and a smaller temperature increase of +17.1°C was observed during the 17 hours preceding the 23:43 MST (6:43 UTC) seismic event at Gull Lake. Hourly averaged wind speeds observed near Pigeon Lake generally increased on January 1 from 7.4 to 11.8 km/hr while veering from South to West (Figure S5b); in contrast, winds near Gull Lake decreased throughout the day from 8.3 to 2.6 km/hr while generally blowing from the South (Figure S5b).

Placed into larger regional and temporal contexts, Alberta Agriculture and Forest data indicate that temperatures prior to the seismic events of January 1 were both unusually cool and arid. Historically, similarly low 7-day average temperatures have been observed once every 6-12 years in this area of Alberta (Figure S6), and precipitation totals during the month preceding the seismic events (Figure 10) were either low (Lac Ste. Anne; observed once in 6-12 years) or moderately low (Pigeon and Gull lakes; observed once in 3-6 years). In contrast, soil moisture conditions (Figure S7) were either near normal (Pigeon and Gull lakes) or above normal (Lac St. Anne) as a result of a relatively wet summer.

Following the seismic events of January 1, a second abrupt warming was observed on January 13 2018. As in the case for the January 1 warming, the January 13 warming was preceded by a ~3-day long period of intense cold (Figure 9), with temperatures ranging between -34.9°C and -20.6°C and averaging -26.2°C. Beginning at 22:00 MST on January 12, temperatures warmed from -27.2°C to +2.8°C (a change of +30.0°C) over a 16 hour period. During this warming interval, hourly averaged wind speeds increased from near still conditions to approximately 20 km/hr while veering from South to West (Figure S5).

4.2 Lake Conditions Prior to January 1 2018

Lake levels prior to the January 1 seismic events, recorded by the Water Survey of Canada, are shown in Table 2. The level recorded for Lac Ste. Anne on the morning of January 1 2018 was 0.380 m higher than the long-term average, while levels recorded for Pigeon and Gull lakes were 0.331 m and 0.068 m below their respective averages; the most recent measurements for these two lakes were taken approximately two months prior to the seismic events.

Table 2. Comparison of average lake levels with levels measured prior to the seismic events.

Lake	Average Level (m); Measurement Interval	Most Recent Level (m); Date of Measurement	Departure (m)
Lac Ste. Anne	722.816; 1933-2018	723.196; 2018/01/01	+0.380
Pigeon Lake	849.921; 1972-2017	849.590; 2017/11/02	-0.331
Gull Lake	898.962; 1938-2017	898.894; 2017/10/31	-0.068
Wabamun Lake	724.318; 1915-2018	724.616; 2018/01/01	+0.298

5 Discussions

5.1 Meteorological Factors Influencing the Generation of Icequakes and Ice-jacking

Abnormal meteorological and hydrological conditions occurred prior to the seismic event on January 1. Firstly, there was a sustained period of extreme cold and rapid freezing of both lake ice and ground surface (Figure 9 & S6). This was followed by a rapid warming period, which saw the daily minimum and maximum air temperatures increase by as much 25-30°C within a 24 hour period (Figure 9). While temperature swings of this magnitude are not uncommon, the coupling of this observation with cool and arid conditions is rare: similar low 7-day average temperatures are observed once every 6-12 years (Figure S6), and similar snow precipitation preceding the seismic events (Figure 10) were either low (Lac Ste. Anne; once in 6-12 years) or moderately low (Pigeon and Gull lakes; once in 3-6 years). Thus, this rapid change in atmospheric temperature was expressed directly to ice due to the near-absence of an insulating snow cover (Figure 10) that would normally buffer large temperature changes.

Based on our observations, we conjecture that the stress of expanding ice was accommodated in two forms: 1) an initial catastrophic rupture of the lake ice that triggered the

M_L 2.0 icequakes recorded at numerous large lakes in west-central Alberta forming pressure/ice ridges, and 2) slower creep occurred as a result of ice-jacking which expressed itself in the form of growing pressure/ice ridges, shoreline ground deformation and damage to infrastructure. Ice-jacking, as defined here, is the cyclic warming and expansion of ice, followed by contraction as the temperature repeatedly rises and falls (e.g., Xanthakos et al., 1994). This process can be diurnal, or episodic depending on the prevailing freezing-warming weather cycles. The weak tensile strength of cooling ice results in cracks (or leads) which become water-filled and freeze, thereby adding new ice to the system. All the while ice creeps shoreward during warming periods, and the lateral stress is accommodated by sustained deformation of the frozen ground layer. This process repeats until the exchange of heat between air and ice is buffered by an insulating snow cover.

This conjecture is corroborated by the near simultaneous observation of brittle ice failures (icequakes) recorded in central Alberta (Figure 1), meteorological conditions consistent with other icequake cases documented (Hamaguchi et al., 1977; Hamaguchi & Goto, 1978; Goto et al., 1980), the observation of Alberta icequakes only at lakes exhibiting these conditions (Figures 9,10,S6,S7), and the continuation of ground deformation and ice ridge building during the second warming event (starting January 13).

5.2 Anticipated Thermal Expansion of Lake Ice

In response to the rapid rise in air temperature during the course of 24 hours on January 1, lake ice underwent rapid thermal expansion. If we assume that this expansion radiated outward from the central parts of the lakes toward shore, back-of-the-envelope calculations suggest that the expansion could have been as much as 6-7 m (Table 3). In contrast, the length of the limbs in near-vertical folds at Lac Ste. Anne indicated expansion closer to 3-4 m. However, more rigorous modeling (as presented next) could better account for these discrepancies.

Table 3. Theoretical amount of ice expansion expected during the rapid warming period of January 1 2018 on Lac Ste. Anne.

Expansion Parameter	Value
C – coefficient of ice expansion (% volume change per °C)	50×10^{-6}
r – radius of Lac Ste. Anne (km)	~5.0
ΔT – Change in temperature over 24 hour period (°C)	+25-30
Δd_t – Anticipated thermal expansion at lake edge = C*R* ΔT (m)	6.0-7.5
Δd_e – Measured shortening at lake edge (m)	3.0-4.0

To more thoroughly examine the impact of air-temperature driven changes in lake ice thermal expansion, we employed a simple 1D temperature diffusion model. This model is applied to two scenarios. In the first, air temperature changes act directly on a bare ice layer (0.4 m thick in all model runs); in the second, air temperatures act upon an overlying snowpack that insulates the ice (0.3 m thick). In both cases, the bottom of the ice layer is held at a constant 0°C to mimic contact with lake water, and the temperature at the top of the ice or snow is assumed equal to the (time-varying) air temperature. A description of the model and relevant parameter values are presented in the Supplementary Materials.

Both model scenarios described above are first subjected to a 24 hour period of warming, with an air temperature that increases linearly from -29°C to -2°C. Modelled warming periods are similar to temperatures observed at Lac Ste. Anne on January 1-2 2018 (Figure 9). This warming is then followed by an extra 5-day period in which air temperatures are held constant (-2°C), in order to examine further adjustment of ice temperature profiles. For both scenarios, the model is initialized by allowing the temperature profile within the ice or snow to equilibrate to a steady air temperature of -30°C before warming.

Modelled temperature profiles from the snow-free and snow-covered scenarios are shown in Figure 11. Comparison of these two figures shows that ice temperature changes during the 24 hours of warming are strongly influenced by the absence or presence of snow cover. For the case with no snow, the ice surface warms by the full 27°C (as prescribed at the model's upper boundary condition), while the depth-averaged ice temperature increases by 12.5°C. In contrast, for the case with a 0.3 m thick snow cover, the temperature increase largely occurs within the layer of snow, and as a result the upper ice surface warms by just 3.5°C and the depth-averaged ice temperature by only 1.4°C.

If we assume that thermal expansion of the lake ice is due to depth-averaged changes in ice temperature and occurs over a lateral distance of 5.0 km (similar to the half-width of Lac Ste. Anne), these modelled temperature changes correspond with lateral thermal expansions of 3.1 m and 0.4 m, respectively, for the snow-free and snow-covered scenarios described above. The modelled expansion for the snow-free case thus matches well with the observed expansion of 3-4 m at Lac Ste. Anne (Table 3).

After the initial 24 hour period of prescribed warming, lake ice in the snow-free scenario largely equilibrates with the steady -2°C air temperature within one model day (see the "48 hr" profile in Figure 11a). In contrast, the presence of snow cover slows equilibration by several days (Figure 11b). Net depth-averaged temperature changes for the two scenarios at the end of the 6-day runs are +14.4°C and +8.3°C, respectively, corresponding to lateral thermal expansions of +3.6 m and +2.1 m.

Taken together, these model runs demonstrate that the presence of snow cover decreases both the magnitude and rate of thermal expansion of lake ice. The reason for this is twofold: first, snow has a lower thermal diffusivity than ice, and thus acts as an insulator; second, when snow is present, the greatest temperature changes occur in snow (Figure 11), which is relatively weak as compared to stronger ice. As a result, a rapid warming event that occurs at a time when snow cover is thin or absent would generate greater stresses via thermal expansion than would a similar warming event at a time of thick snow cover; these stresses would also develop at a much greater rate. If these stresses increase at a rate too large to be accommodated by creep deformation of the lake ice and shoreline materials upon which the lake ice bears, they would build until they exceed the yield strength, at which brittle failure would occur. For this reason, the thin-to-absent snow cover on Lac Ste. Anne, Pigeon Lake, and Gull Lake during this time interval (e.g., Figures 4-7 & S3), and warm convective winds likely played a significant role in the development of the observed icequakes.

5.3 Lake-Bottom Factors Influencing Ice and Ground Deformation

A comparison of lake-bottom profiles provides some insight as to where and why pressure/ice ridges developed on Lac Ste. Anne on January 1, and why some parts of the lake experienced significant ground deformation and others did not. Pressure/ice ridges appeared to have developed in shallow parts of the lake, near shore. Particularly, pressure/ice ridges formed in areas with longitudinal, parallel wavy bedforms where crests of ridges were proximal to the undersurface of the ice (e.g. Figure 8 transect 1 & Figure 12). In these areas of shallow lake depths, ice appears to have frozen directly to the lake bed (Figure 4a) – providing mechanical resistance to thermal expansion, and causing ice to rupture off shore rather than completely transmitting stress laterally onto shore (Figure 13 a,b). Conversely, in areas where the lake is deeper near-shore, the lake ice was not frozen to its bed and the stresses generated by the warming/expanding ice on January 1 were transferred directly to the frozen ground onshore (Figure 13 c,d).

In addition to differences in lake bed morphology, the shoreline at Lac Ste. Anne may have been more susceptible to the stresses of expanding ice as a result of higher amounts of precipitation than in previous years (Figure S7), which could contribute to weaker soil conditions near shore. This certainly is the case at the Thibeault site where marshy, saturated ground was severely impacted by the ice. A higher-than-normal lake level (like at Lac Ste. Anne, Table 2) would also result in deep water at the shoreline, preventing lake ice freezing to its bed, thereby reducing or eliminating the amount of shoreline basal resistance to the thermal expansion of ice. This may explain why there was widespread impact to shorelines along both Lac Ste. Anne and Wabamun Lake.

5.4 The Seismogenic Potential of Medium Sized Lakes

Based on prior arguments, it is reasonable to conclude that the recorded seismic events were lake-associated icequakes. Here we determine if thermal expansion of lake ice is capable of producing an **M** 2.0 seismic event. Figure 4 shows large pressure/ice ridges across the lake ice, including both overlapping ridges and folded ones. However, these figures do not demonstrate whether failure was near-instantaneous, releasing potentially damaging seismic energy, or occurred aseismically over an extended period. Given these considerations, we determine the length L of ice that must have ruptured to produce the observed icequake magnitude (**M** 2.0). The moment magnitude **M** of an earthquake is given by

$$\mathbf{M} = (2/3)(\log_{10}(M_O) - 9.05), \quad \text{(Eq. 1)}$$

where M_O is the seismic moment (in units of Nm): a quantity that is proportional to the amount of energy released by a seismic event (Hanks & Kanamori, 1979). The previously observed overlapping ridges are created by shear failure of the ice, followed by over- and underthrusting of the ice sheets. This is similar to shear failure of existing faults in the earth which have well studied moment tensors from which the kinetically released energy can be computed (Julian et al., 1998). The seismic moment M_O for shear failure is given by

$$M_O = \mu A d, \qquad \text{(Eq. 2)}$$

where μ is the shear modulus (3.8 GPa for ice), A is the slip area, and d is the average displacement of slip area. The slip area is given by A = L d, with L representing the fault length. For over/under-thrusting to occur, the ice must rupture across its entire thickness h. Thus, the amount of slip displacement d is given by

$$d = h/\sin(\theta), \qquad \text{(Eq. 3)}$$

with θ indicating the rupture angle with respect to the direction of the maximum stress (horizontal in this case). For reference, an angle of θ=90° indicates a vertical shearing of the ice. We note that Schulson et al. (2006) found a shearing angle of θ=27° for sea ice. Combining equations 1-3 produces

$$\mathbf{M} = (2/3)(\log_{10} (\mu L h^2/ \sin^2(\theta)) - 9.05). \qquad \text{(Eq. 4)}$$

Inverting for the length L yields

$$L = 10^{1.5\mathbf{M}+9.05} \sin^2(\theta)/ (\mu h^2). \qquad \text{(Eq. 5)}$$

Given a measured ice thickness h = 0.4 m and observed moment magnitude of **M** 2.0, equation 5 requires a rupture length of L = 383 m (and a slip distance of d = 88 cm). In general, more vertical rupture angles θ will require larger rupture lengths L to produce a similar magnitude event. For example, ice rupture lengths of L = 1.8 km would be required to produce a **M** 2.0 event with subvertical ice shearing. Overall, these results are consistent with overnight pressure/ice ridge and ice folding at Pigeon Lake and Lac Ste. Anne. For example, numerous sets of pressure/ice ridges were observed on both lakes, extending for hundreds of metres with metres (3-4 m) of displaced ice following the first warming period (Figures 4 & 12). At Pigeon Lake, one such pressure/ice ridge on the eastern portion of the lake displayed clear evidence of periodic under/over-thrusting behavior (Figure 4b).

Taken to its extreme limit, we also consider the maximum possible magnitude **M** a lake in central Alberta could theoretically produce – given the unlikely scenario that the entire circumference of the lake ruptures simultaneously. Lac Ste. Anne has an approximate radius of 5 km, leading to a total rupture length L = 31.4 km. Substituting this into equation (4) with a thickness of h = 0.4 m and shear angle of θ = 27°, suggests that this lake could host an icequake event as large as **M** 3.3.

We note that this rupture analysis is only applicable for shear failure modes that result in under/over-thrusting behaviour and not folded pressure ridges formed instead by tensile failure. This tensile failure leads to fracture surfaces that are perpendicular to the plane of the lake ice and thus of smaller displacements d. Unfortunately, the corresponding moment tensor is not identical to those of well-studied earthquakes (mode II) since the lake ice moves apart by a combination of tensile (mode I) failure and also includes a rotational motion. Since tensile failure tends to be more energetic than shear failure (Van der Baan et al., 2016) under otherwise equal circumstances (stress drops and fracture lengths), it seems reasonable to assume that an **M** 2.0 event corresponds to a similar rupture length L in case of a folded ridge.

6 Conclusions

In conclusion we find that the seismic events of the evening of January 1-2 2018 were likely icequakes caused by sudden brittle failure of ice due to thermal expansion stresses. The occurrence of these icequakes nearly simultaneously on independent lakes bolsters this interpretation. Factors including minimal snow cover, high lake levels, an abrupt period of dramatic warming, and warm winds all contributed to the expression of these events. While ground shaking was observed and consistent with multiple lines of reasoning, it likely was of insufficient intensity to cause damage. Instead, onsite observations of ground deformations are consistent with continued (aseismic, creeping) ground deformations for a period (of weeks) after the initial brittle failures. We suggest that the coupling of expanding ice to the shoreline in the production of ground deformation is controlled by ice bed conditions (frozen or floating), lake bathymetry, and soil conditions. This reasoning is supported by a second warming period during which the amplitude of observed ground deformation and pressure/ice ridge formations doubled. Simple seismic magnitude relationships suggest that frozen lakes in Alberta (and elsewhere) can represent a source of moderate magnitude seismicity, given the proper circumstances.

7 Acknowledgements

We would like to thank the numerous landowners who shared information with us: their time, photos, stories, and access to property. We would like to thank Don Davidson for insightful conversations that were helpful in constructing this manuscript. As well, we would like to thank Don Meredith and Neil Fleming for providing ground photographs and field observations at Wabamun Lake and Neil Keown of Spectre UAV for sharing his drone flight data. We would also like to thank Javad Yusifbayov for assistance during field visits. Seismological data are available online at the Incorporated Research Institutions for Seismology (https://www.iris.edu/hq/). Lake level data were extracted from the Environment and Climate Change Canada Historical Hydrometric Data web site, https://wateroffice.ec.gc.ca/mainmenu/historical_data_index_e.html (downloaded May and June, 2018). Alberta weather data were provided by Alberta Agriculture and Forestry, Alberta Climate Information Service (ACIS), https://agriculture.alberta.ca/acis (downloaded May and June, 2018). For each township, meteorological data were downloaded from the township data viewer webpage (https://agriculture.alberta.ca/acis/township-data-viewer.jsp). Additional weather/lake level data were provided by Amber Brown and Samantha Hussey (Environmental and Climate Change Canada), and Ralph Wright (Alberta Agriculture and Forestry). Lastly, we would like to thank Richard Aster and Rene Barendregt for their reviews of this manuscript.

References

Amundson, J.M., Truffer, M., Lüthi, M.P., Fahnestock, M., West, M., & Motyka, R.J. (2008). Glacier, fjord, and seismic response to recent large calving events, Jakobshavn Isbræ, Greenland. *Geophysical Research Letters*, 35(22), L22501, doi:10.1029/2008GL035281.

Anandakrishnan, S. & Bentley, C.R. (1993). Micro-earthquakes beneath Ice Streams B and C, West Antarctica: observations and implications. *Journal of Glaciology*, 39(133), 455-462, doi: 10.3189/S0022143000016348.

Annan, A. P., & Davis, J. L. (1977). Impulse radar applied to ice thickness measurements and freshwater bathymetry. *Geological Survey of Canada, Report of Activities Paper*, 117-124.

Assatourians, K., & Atkinson, G. (2010). Database of processed time series and response spectra data for Canada: An example application to study of 2005 MN 5.4 Riviere du Loup, Quebec, earthquake. *Seismological Research Letters*, *81*(6), 1013-1031, doi: 10.1785/gssrl.81.6.1013.

Aster, R. C., & Winberry, J. P. (2017). Glacial seismology. *Reports on Progress in Physics*, *80*(12), 126801.

Atkinson, G. M., & Boore, D. M. (2006). Earthquake ground-motion prediction equations for eastern North America. *Bulletin of the Seismological Society of America*, *96*(6), 2181-2205.

Atkinson, G. M., & Kaka, S. I. (2007). Relationships between felt intensity and instrumental ground motion in the central United States and California. *Bulletin of the Seismological Society of America*, *97*(2), 497-510, doi: 10.1785/0120060154.

Atkinson, G. M., Eaton, D. W., Ghofrani, H., Walker, D., Cheadle, B., Schultz, R., ... & Liu, Y. (2016). Hydraulic fracturing and seismicity in the Western Canada Sedimentary Basin. *Seismological Research Letters*, *87*(3), 631-647, doi: 10.1785/0220150263.

Atkinson, G. M., & Assatourians, K. (2017). Are ground-motion models derived from natural events applicable to the estimation of expected motions for induced earthquakes?. *Seismological Research Letters*, *88*(2A), 430-441, doi: 10.1785/0220160153.

Barosh, P. J. (2000). Frostquakes in New England. *Engineering geology*, *56*(3-4), 389-394, doi: 10.1016/S0013-7952(99)00092-7.

Battaglia, S. M., Changnon, D., Changnon, D., & Hall, D. (2016). Frost Quake Events and Changing Wintertime Air Mass Frequencies in Southeastern Canada. doi: 10.13140/RG.2.2.22351.48803

Bradley, C. C. (1948). Mendota [Wisconsin] quake [1/15/48]. *American Journal of Science*, *246*(6), 390.

Moorman, B. J., & Michel, F. A. (1997). Bathymetric mapping and sub-bottom profiling through lake ice with ground-penetrating radar. *Journal of Paleolimnology*, *18*(1), 61-73, doi: 10.1023/A:1007920816271.

Cui, L., & Atkinson, G. M. (2016). Spatiotemporal variations in the completeness magnitude of the Composite Alberta Seismicity Catalog (CASC). *Seismological Research Letters*, *87*(4), 853-863, doi: 10.1785/0220150268.

Dobretsov, N. L., Psakh'e, S. G., Ruzhich, V. V., Popov, V. L., Shil'ko, E. V., Granin, N. G., ... & Starchevich, Y. (2007, March). Ice cover of Lake Baikal as a model for studying tectonic processes in the Earth's crust. In *Doklady Earth Sciences* (Vol. 413, No. 1, pp. 155-159). Nauka/Interperiodica, doi: 10.1134/S1028334X07020018.

Dobretsov, N. L., Ruzhich, V. V., Psakhie, S. G., Chernykh, E. N., Shilko, E. V., Levina, E. A., & Ponomareva, E. I. (2013). Advance in earthquake prediction by physical simulation on the baikal ice cover. *Physical Mesomechanics*, *16*(1), 52-61, doi: 10.1134/S1029959913010062.

Don Meredith Outdoors Blog (2018) URL: https://donmeredith.wordpress.com/2018/01/26/the-power-of-lake-ice/

Ghofrani, H., & Atkinson, G. (2018). Distinguishing Cryoseisms from Earthquakes in Alberta, Canada. *Canadian Journal of Earth Sciences*, doi: 10.1139/cjes-2018-0089.

Hamaguchi, H., Suzuki, Z., Koyama, J., & Goto, K. (1977). A Study on Ice Faulting and Icequake Activity in the Lake Suwa,(1) Preliminary Field Observations. *Science reports of the Tohoku University. Ser. 5, Geophysics*, *24*(1), 43-54.

Hamaguchi, H., & Goto, K. (1978). A study on ice faulting and icequake activity in the Lake Suwa,(2) temporal variation of m-value. *Science reports of the Tohoku University. Ser. 5, Geophysics*, *25*(1), 25-38.

Hanks, T.C., Kanamori, H. (1979). A moment magnitude scale. *Journal of Geophysical Research: Solid Earth, 84(B5)*, 2348-2350, doi: 10.1029/JB084iB05p02348.

Goto, K., Hamaguchi, H., & Wada, Y. (1980). A study on ice faulting and icequake activity in the Lake Suwa.(3) Icequake activity and thermal stresses in ice plate. *The science reports of the Tohoku University. Fifth series, Tohoku geophysical journal*, *27*(1), 27-37.

Government of Canada Ice Glossary: https://www.canada.ca/en/environment-climate-change/services/ice-forecasts-observations/latest-conditions/glossary.html

Global News, (2018). Experts still looking into what caused Monday's seismic event in Alberta. https://globalnews.ca/news/3943723/alberta-beach-seismic-event-what-is-ice-quake/

Gu, Y. J., & Shen, L. (2012). Microseismic noise from large ice-covered lakes?. *Bulletin of the Seismological Society of America*, *102*(3), 1155-1166, doi: 10.1785/0120100010.

Julian, B. R., Miller, A. D., & Foulger, G. R. (1998). Non-double-couple earthquakes 1. Theory. *Reviews of Geophysics*, *36*(4), 525-549, doi: 10.1029/98RG00716.

Lermo, J., & Chávez-García, F. J. (1993). Site effect evaluation using spectral ratios with only one station. *Bulletin of the seismological society of America*, *83*(5), 1574-1594.

Leung, A. C., Gough, W. A., & Shi, Y. (2017). Identifying Frostquakes in Central Canada and Neighbouring Regions in the United States with Social Media. In *Citizen Empowered Mapping* (pp. 201-222). Springer, Cham.

Mahani, A. B., & Kao, H. (2017). Ground Motion from M 1.5 to 3.8 Induced Earthquakes at Hypocentral Distance< 45 km in the Montney Play of Northeast British Columbia, Canada. *Seismological Research Letters*, *89*(1), 22-34, doi: 10.1785/0220170119.

Makkonen, L., Törnqvist, J., & Kuutti, J. (2010). Vibrations of buildings induced by thermal cracking of lake ice. In *20th IAHR International Symposium on Ice* (pp. 1-11).

Nikonov, A. A. (2010). Frost quakes as a particular class of seismic events: Observations within the East-European platform. *Izvestiya, Physics of the Solid Earth*, *46*(3), 257-273, doi: 10.1134/S1069351310030079.

Nigam, N. C., & Jennings, P. C. (1969). Calculation of response spectra from strong-motion earthquake records. *Bulletin of the Seismological Society of America*, *59*(2), 909-922.

Nishio, F. (1983). Studies on thermally induced fractures and snowquakes of polar snow cover, *Memoirs of National Institute of Polar Research*, 14, 48 p.

Novakovic, M., & Atkinson, G. M. (2015). Preliminary evaluation of ground motions from earthquakes in Alberta. *Seismological Research Letters*, *86*(4), 1086-1095, doi: 10.1785/0220150059.

Podolskiy, E. A., & Walter, F. (2016). Cryoseismology. *Reviews of Geophysics*, *54*(4), 708-758, doi: 10.1002/2016RG000526.

Qamar, A. (1988). Calving icebergs: a source of low-frequency seismic signals from Columbia Glacier, Alaska. *Journal of Geophysical Research*, 93(B6), 6615-6623, doi: 10.1029/JB093iB06p06615.

Ruzhich, V. V., Psakhie, S. G., Chernykh, E. N., Bornyakov, S. A., & Granin, N. G. (2009). Deformation and seismic effects in the ice cover of Lake Baikal. *Russian Geology and Geophysics*, *50*(3), 214-221, doi: 10.1016/j.rgg.2008.08.005.

Schulson, E. M., Fortt, A. L., Iliescu, D., & Renshaw, C. E. (2006). Failure envelope of first-year Arctic sea ice: The role of friction in compressive fracture. *Journal of Geophysical Research: Oceans*, *111*(C11), doi: 10.1029/2005JC003235.

Schultz, R., & Stern, V. (2015). The Regional Alberta Observatory for Earthquake Studies Network (RAVEN). *CSEG Recorder*, *40*(8), 34-37.

Schultz, R., Stern, V., Gu, Y. J., & Eaton, D. (2015). Detection threshold and location resolution of the Alberta Geological Survey earthquake catalogue. *Seismological Research Letters*, *86*(2A), 385-397, doi: 10.1785/0220140203.

Schultz, R., Wang, R., Gu, Y. J., Haug, K., & Atkinson, G. (2017). A Seismological Overview of the Induced Earthquakes in the Duvernay play near Fox Creek, Alberta. *Journal of Geophysical Research: Solid Earth*, doi: 10.1002/2016JB013570.

Schultz, R., Atkinson, G., Eaton, D. W., Gu, Y. J., & Kao, H. (2018). Hydraulic fracturing volume is associated with induced earthquake productivity in the Duvernay play. *Science, 359*(6373), 304-308, doi: 10.1126/science.aao0159.

Siddiqqi, J., & Atkinson, G. M. (2002). Ground-motion amplification at rock sites across Canada as determined from the horizontal-to-vertical component ratio. *Bulletin of the Seismological Society of America*, *92*(2), 877-884.

Stern, V. H., Schultz, R. J., Shen, L., Gu, Y. J., & Eaton, D. W. (2013). Alberta earthquake catalogue, version 1.0: September 2006 through December 2010. *Alberta Geological Survey Open-File Report*, *15*, 36p.

Stuart, G., Murray, T., Brisbourne, A., Styles, P., & Toon, S. (2005). Seismic emissions from a surging glacier: Bakaninbreen, Svalbard. *Annals of Glaciology*, 42, 151-157, doi: 10.3189/172756405781812538.

Van der Baan, M., Eaton, D. W., & Preisig, G. (2016). Stick-split mechanism for anthropogenic fluid-induced tensile rock failure. *Geology*, *44*(7), 503-506, doi: 10.1130/G37826.1.

Wabamun Watershed Management Council Website. (2018) URL: http://www.wwmc.ca/index.php/what-s-new?id=397-january-2018-ice-heave,

Walter, F., Deichmann, N., & Funk, M. (2008). Basal icequakes during changing subglacial water pressures beneath Gornergletscher, Switzerland. *Journal of Glaciology*, 54(186), 511-521, doi: 10.3189/002214308785837110.

Wood, H. O., & Neumann, F. (1931). Modified Mercalli intensity scale of 1931. *Bulletin of the Seismological Society of America*, *21*(4), 277-283.

Xanthakos, P. P., Abramson, L. W., & Bruce, D. A. (1994). *Ground control and improvement*. New York, John Wiley. p. 737.

Figure Captions

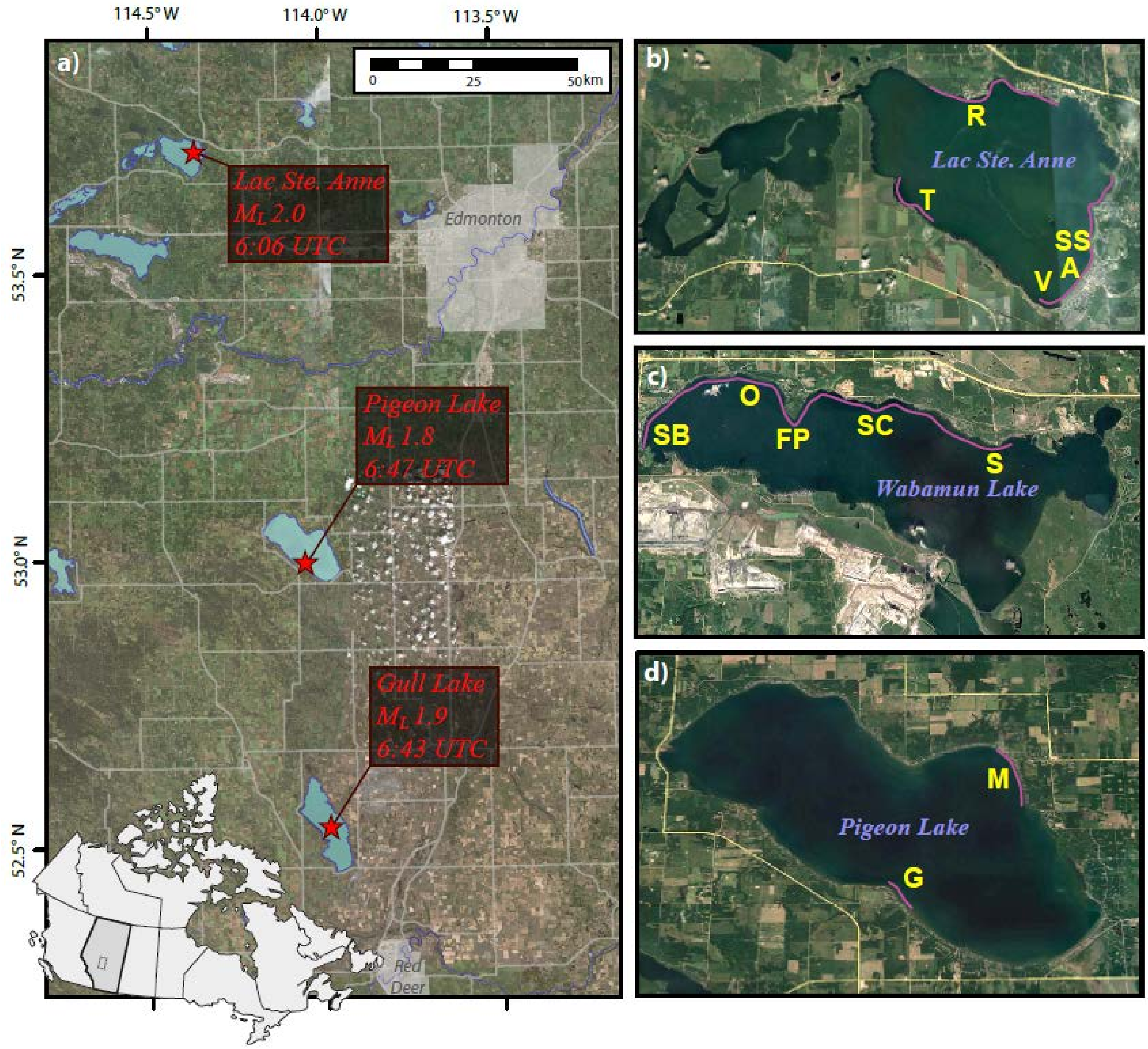

Figure 1. Maps of the study area. (a) Locations of three seismic events (red stars) detected during the evening of January 1-2 2018, associated text boxes describe their details (23:00 MST = 6:00 UTC). Lakes (blue area), nearby cities (grey areas), and roadways (grey lines) are shown for geographic reference. Inset: political boundaries and the study location within Canada. (b-d) Locations of onsite observations made at three lakes (labelled in blue). Pink edges along shorelines denote areas with identified ice ridges or ground deformation. Abbreviations are as follows: Pigeon Lake – (M, Mulhurst), (G, Grandview); Wabamun Lake UAV survey – (SB, Seba Beach), (O, Oselia), (FP, Fallis Point), (SC, Scout Camp), (S, Sailing Club); Lac Ste. Anne – (SS, Sunset Beach), (A, Alberta Beach), (V, Val Quentin), (T, Thibeault,), (R, Ross Haven). Not shown are other lakes reporting shoreline impacts, such as Baptiste Lake about 130 km north of Edmonton.

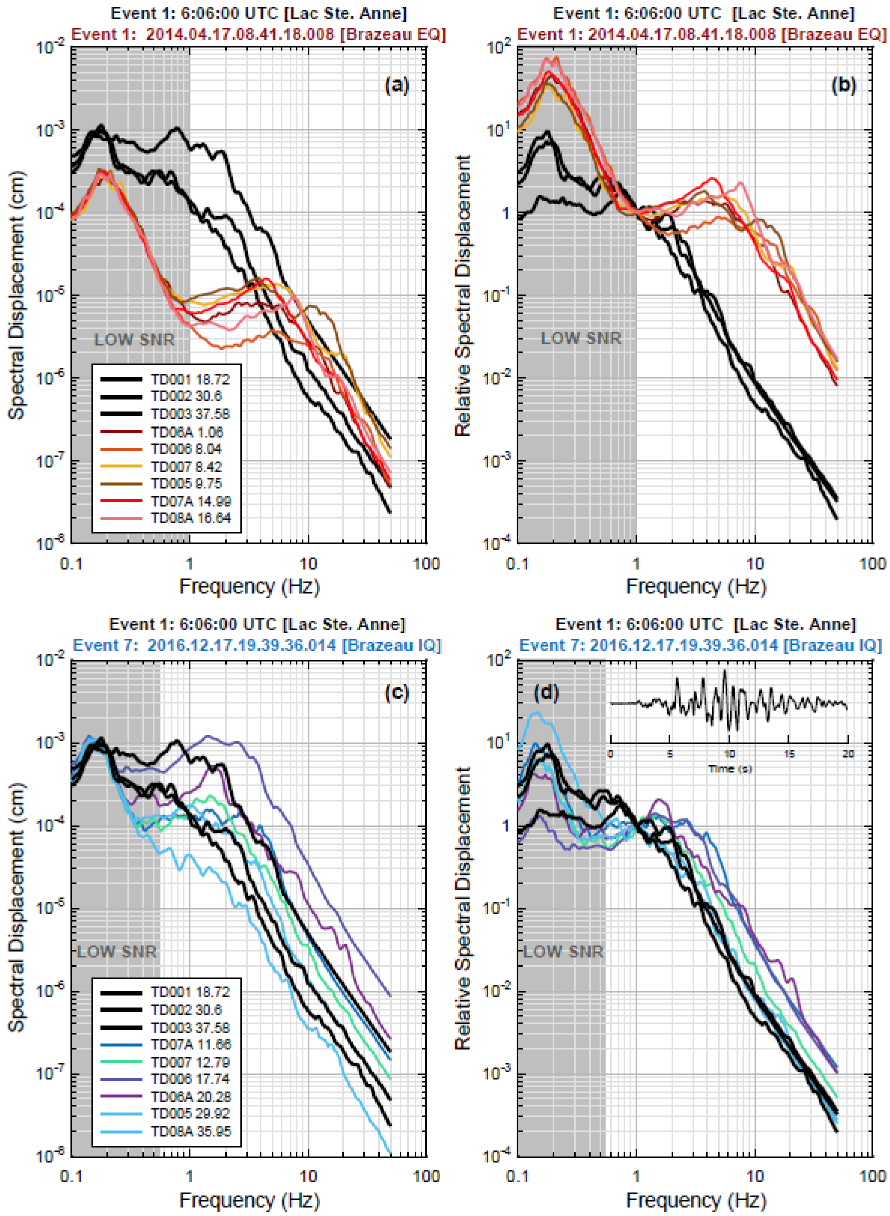

Figure 2. Comparison of seismic event spectra. (a & c) Unscaled and (b & d) scaled response spectra for the Lac Ste. Anne event (geometric mean of horizontal components) versus the natural Brazeau-area earthquake M_L 0.7 (Event 1, a & b) and a Brazeau-area cryoseism M_L 0.4 (Event 7, c & d); scaled spectra have their signals normalized to average unity at 1 Hz. Spectral plots compare a Brazeau earthquake (crimson coloured lines), Brazeau cryoseism (cool coloured lines) and the Lac Ste. Anne event (black lines). Regions of low signal to noise ratio are shaded in grey. Inset seismogram shows vertical velocity waveform data at a nearby station (TD07A). Additional waveform data can be viewed in Figure S2.

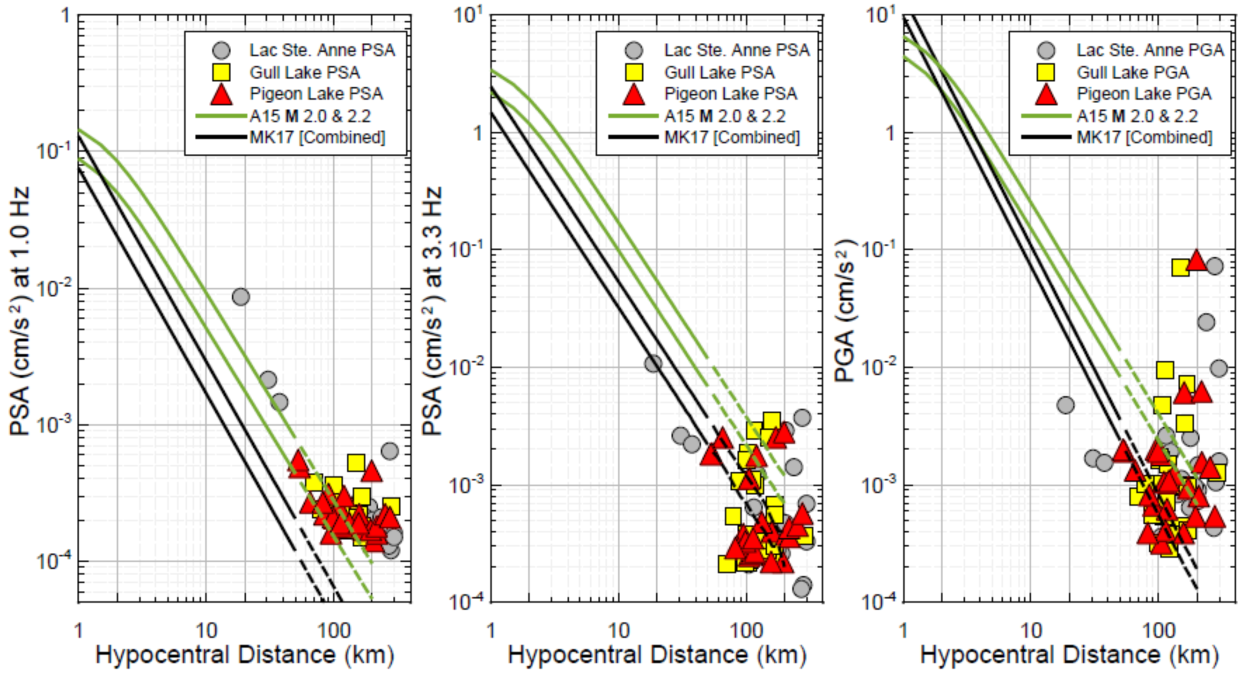

Figure 3. Vertical component ground motions, compared to GMPEs for B/C site condition (Vs30 = 760 m/s). Note that the MK17 and A15 models are only for <50 km (shown as dotted lines beyond 50 km). The green and black lines are A15 and MK17 models (for **M**2.0 and **M**2.2), respectively.

Figure 4. Ice ridges formed on west-central Alberta lakes. (a) ~1.5m high near-vertical offshore ice ridge, with embedded lake boulders. Grandview, Pigeon Lake, January 9 2018. (b) Offshore finger-rafts of over and under-thrust ice slabs, Mulhurst Bay, Pigeon Lake, January 4 2018. (c) ~1.0-1.5 m high, near-vertical, offshore ice ridge, Sunset Beach, Lac. Ste. Anne, January 5 2018. (d) ~2.0-2.5 m high, near-vertical, offshore ice ridge, Sunset Beach, Lac. Ste. Anne, January 18 2018. The ice was about 0.35-0.40 m thick at time of rupture on January 1 2018. (e) ~1.5 m high, onshore, ice ridge, Alberta Beach, Lac. Ste. Anne, January 5 2018. (f) ~1.0 m high, offshore, ice ridge, Seba Beach, Wabamun Lake, January 9 2018. Locations of pictures are annotated in the bottom left of the panels based on acronyms in Figure 1.

Figure 5. Deformed shorelines. (a) 1.0-1.5 m high, thrusted and folded marshy shoreline at the Thibeault site, Lac Ste. Anne on January 5 2018. (b & c) Same location, but taken two weeks after photo (a); the height of thrust increased by at least 1 m. (c) Lake-side view of photo (b), with ~2.5m high near-vertical thrust ridge of frozen marshy ground. Lake ice plunges beneath thrust ridge, and water rises to surface. (d) Thrusted, folded shoreline at Sunset Beach, Lac. Ste. Anne, January 19 2018. Note re-frozen lead (crack) on flat lake ice at the left edge of the photo. (e) Thrusted, folded shoreline and undeformed lake ice adjacent to thrust ridge at Seba Beach, Wabamun Lake, January 7-9 2018. In all photos, note the sparse snow cover. Locations of photos are annotated in the bottom left of the panels based on acronyms in Figure 1.

Figure 6. Inland ground deformations. (a) View of undeformed lake ice in contact with shore, and folded, deformed ground onshore beneath the gazebo structure at the Thibeault site, Lac. Ste. Anne, January 19 2018. (b) Multiple inland ground folds (numbered) at the Thibeault site, Lac. Ste. Anne, January 5 2018. Photo (b) taken 5 days after the icequake, during which time folds grew to about 0.5 m in height. (c & d) Photos taken two weeks later, during which time folds have doubled in height and ruptured. (e & f) Aerial view (UAV imagery) of folded ground at two sites near Seba Beach, Wabamun Lake. Ridges in photo (e) are about 0.3-0.4 m high and 7-13 m long. Ruptures (R) are evident in some of the folds. (f) Ridges in photo (highlighted in yellow) are about 0.4-0.5 m high and 5-8 m long. Locations of pictures are annotated in the bottom left of the panels based on acronyms in Figure 1.

Figure 7. Damage to infrastructure following the icequakes. (a & b) Damaged decking and pillar footings of gazebo structure situated above deformed, folded ground ridge, Thibeault, Lac Ste. Anne. Further damage to structure occurred as folds grew in height over a two-week period (b). Multiple folds are visible in background in left edge of photo (b). (c) Deck deformed and displaced by onshore ice ridge, Lac Ste. Anne. (d) Sheared concrete retaining wall, Seba Beach area, Wabamun Lake. Locations of pictures are annotated in the bottom left of the panels based on acronyms in Figure 1.

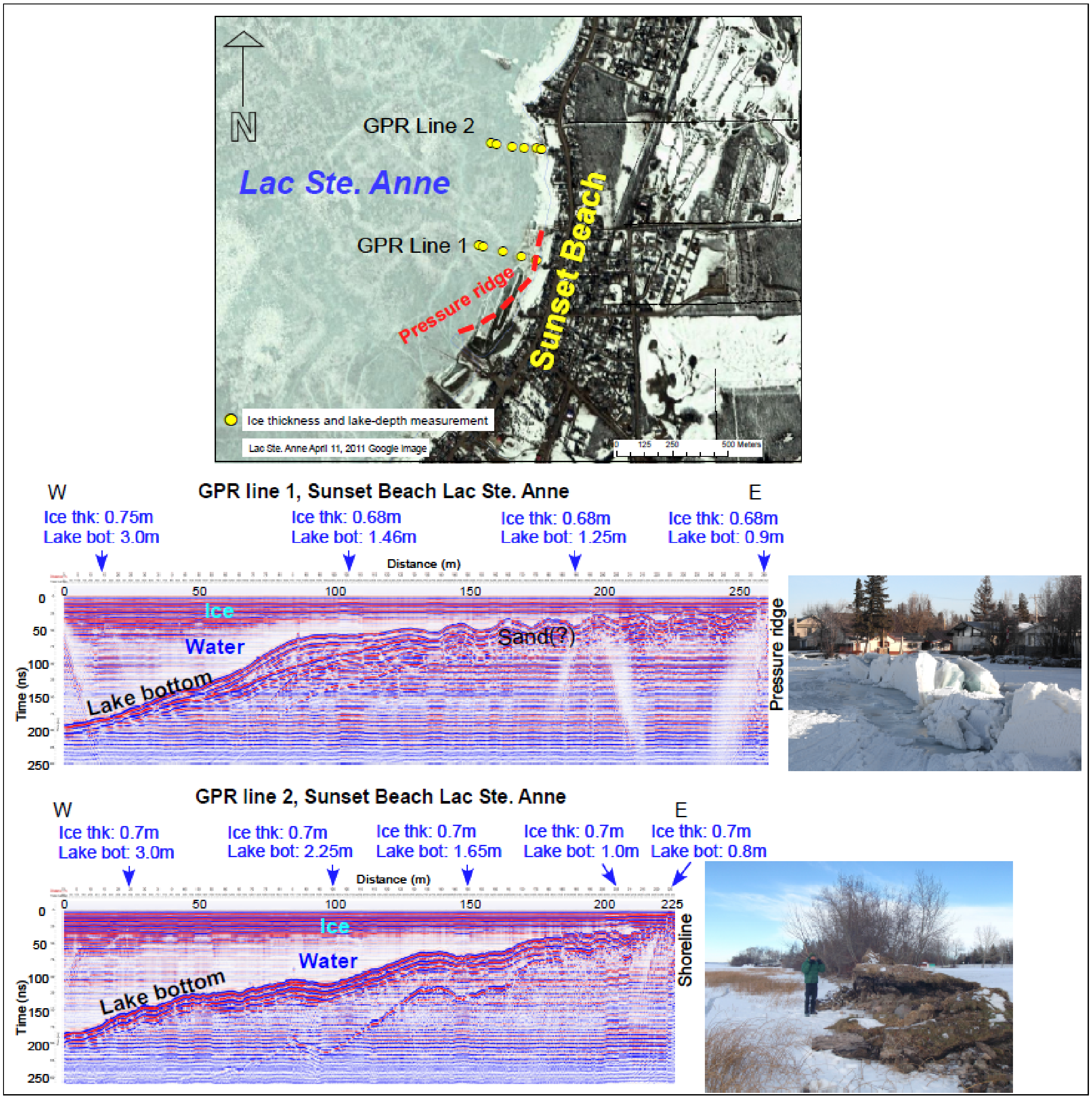

Figure 8. Ground penetrating radar profiles of ice thickness and lake-bottom morphology, Sunset Beach, Lac Ste. Anne. Dashed red line in satellite image marks approximate positon of ice ridge created by the icequake. GPR profiles were surveyed on January 18 2018, about 2.5 weeks after the icequake event. Yellow dots in location figure denote ice-auger borehole site. Blue vertical arrows above GPR profiles denote positions of auger sites, and blue text is sounding information at site. Convoluted wavy forms interpreted as the surface of the lake bottom GPR line 1 correspond to depositional sandy bedforms visible in mid-summer satellite imagery.

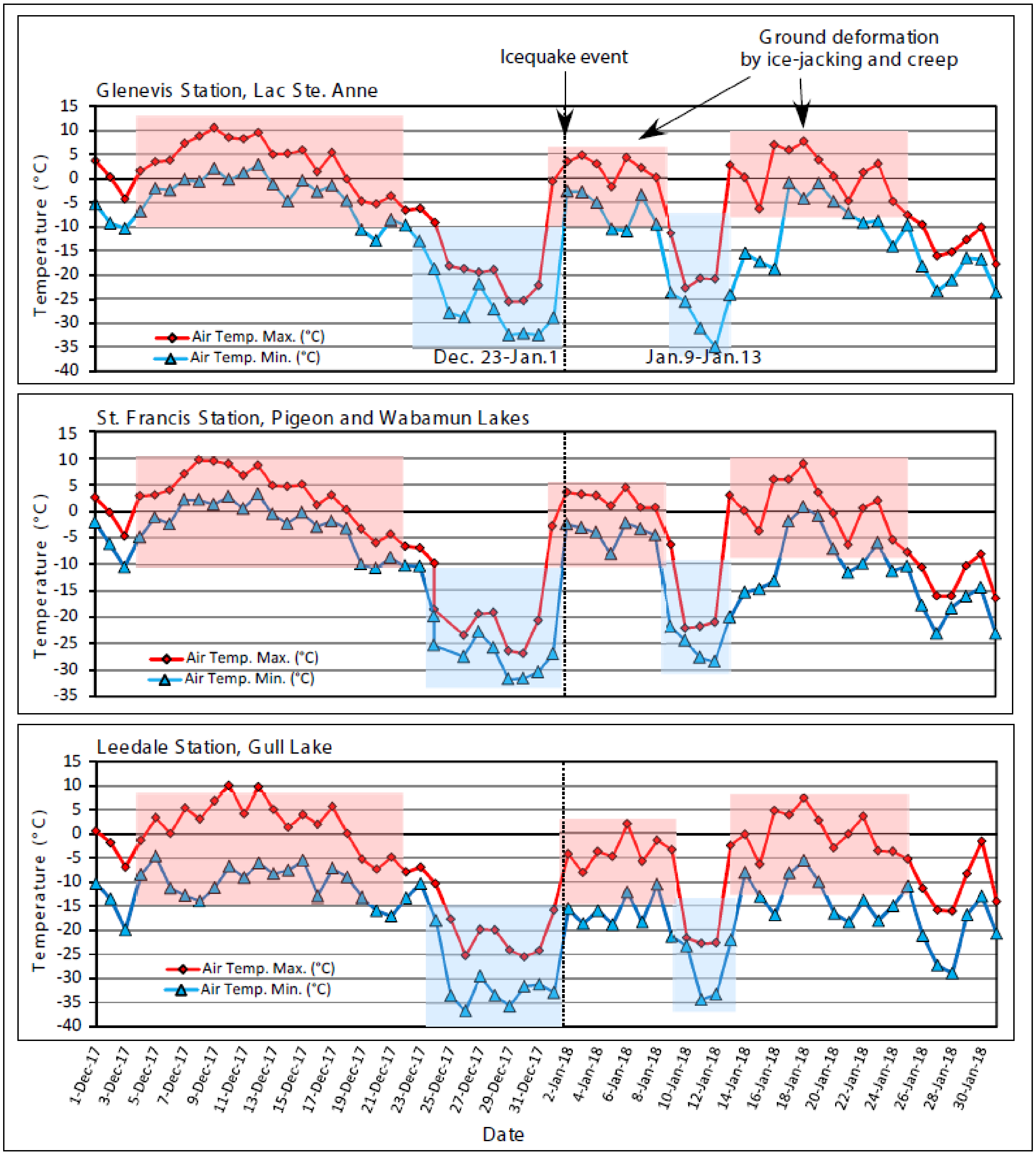

Figure 9. Daily minimum (blue line) and maximum (red line) temperatures in the weeks preceding the icequake event, at the weather stations near relevant lakes. Prolonged cold periods (Blue-shaded areas) around -30°C preceded the seismic event (dashed line) between December 23 and January 1. Red-shaded areas highlight periods of near or above freezing temperatures. Two cycles of rapid temperature drop followed by rapid warming are recorded in the latter part of December 2017 and mid-January 2018.

Data source: http://climate.weather.gc.ca/historical_data/search_historic_data_e.html

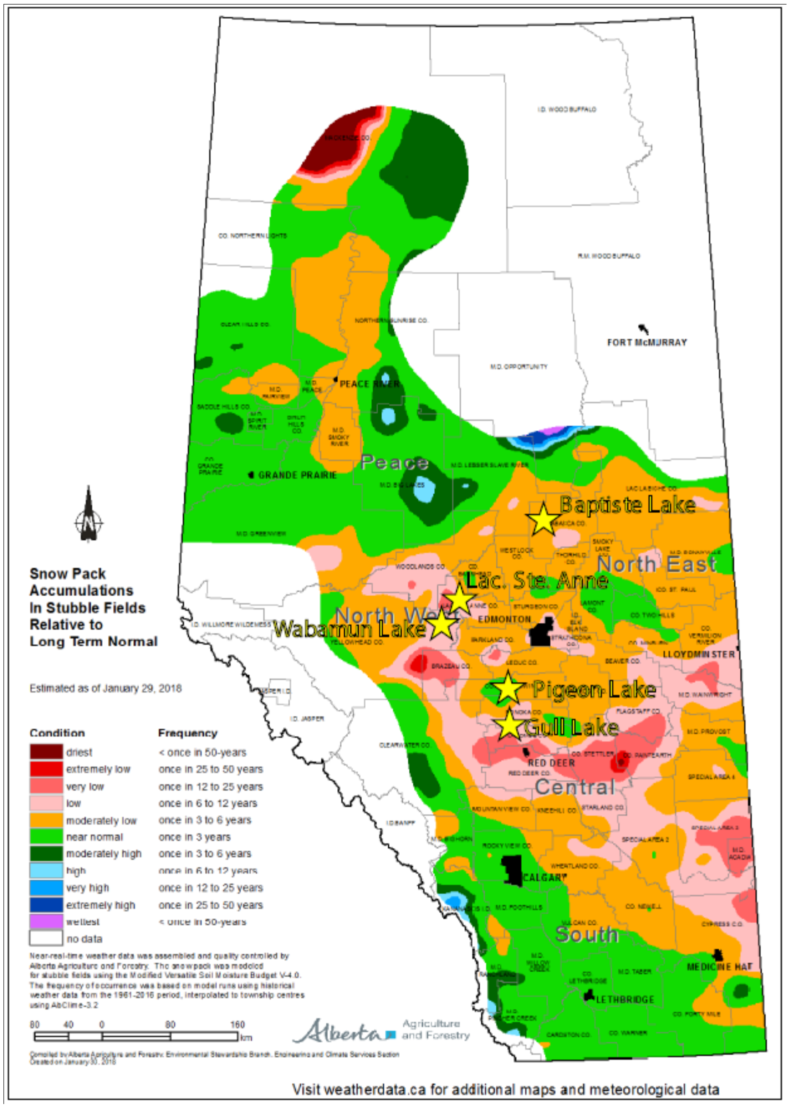

Figure 10. Snow-pack in Alberta relative to normal. Yellow stars show locations of lakes that registered on seismic monitoring stations, or which experienced ice-ridge and/or ground deformation. Gull Lake, Lac. Ste. Anne, Baptiste Lake, and Wabamun Lake are located in areas having very little snow-pack cover relative to long term average. Base map source: http://agriculture.alberta.ca/acis/climate-maps.jsp.

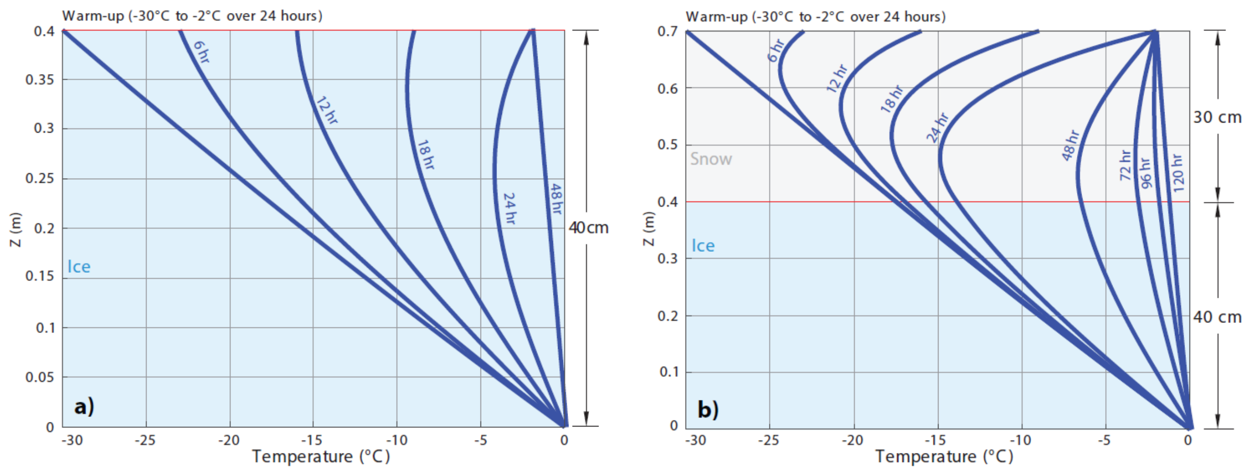

Figure 11. Effects of snow cover on the thermal conductivity of air temperature into ice. (a) Modelled temperature profiles (blue curves) for the warming scenario with a 40 cm thick layer of lake ice (blue area). (b) Modelled temperature profiles (blue curves) for the scenario with a 30 cm thick snowpack (grey area) overlying lake ice (blue area).

Figure 12. Lake-bottom bedforms, approximate positions of pressure/ice ridge, and ground deformation along Sunset Beach, Lac. Ste. Anne. Pressure/ice ridges have developed in areas with shallow shorelines (depicted as longitudinal, parallel to sub-parallel sandy depositional bedforms beneath shallow water in 2011 Google Earth imagery) where lake ice had frozen to its bed. In areas with steeper shorelines, expanding lake ice floated on water, likely transferring more stress and causing more damage to the shoreline.

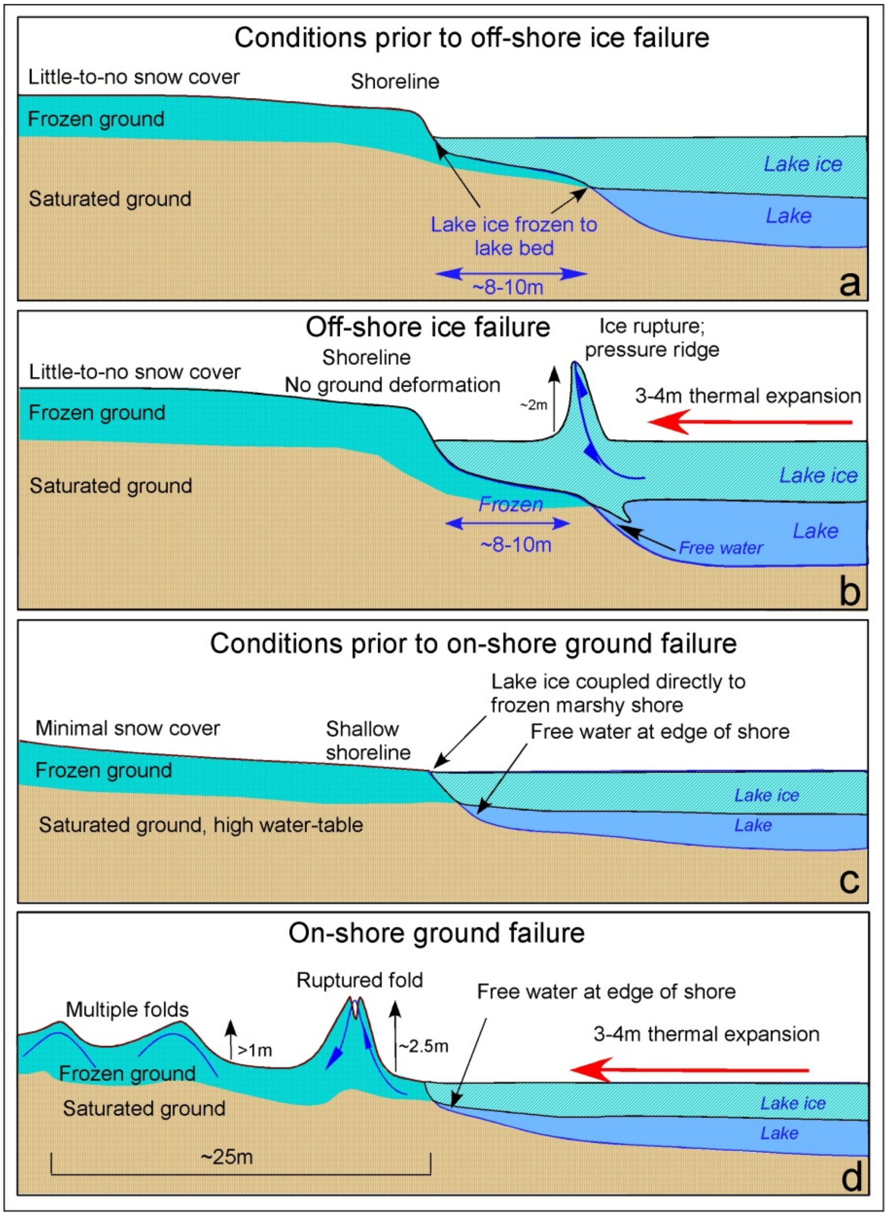

Figure 13. Mechanisms of ice and ground failure during, and subsequent to the icequake event. (a) The process of ice failure is representative of the formation of the off-shore pressure/ice ridges that formed at Pigeon Lake and Lake Ste. Anne. (b) Freezing of the lake ice to its bed near shore during preceding weeks of extreme cold provided sufficient resistance to thermal expansion to cause violent rupture of ice offshore. (c) Elsewhere, where shorelines were relatively steeper, free water existed beneath the ice at shoreline and lake ice was coupled directly to the onshore frozen ground layer and unimpeded by bed resistance. (d) Lateral forces were transferred directly on-land, causing ground displacement in the form of thrusts and folds, especially in areas of wet or marshy ground.